

# Highly Dispersed Metal Nanoparticles in Porous Anodic Alumina Films Prepared by a Breathing Process of Polyacrylamide Hydrogel

Yu-Guo Guo,<sup>†</sup> Jin-Song Hu,<sup>†</sup> Han-Pu Liang,<sup>†</sup> Li-Jun Wan,<sup>\*</sup> and Chun-Li Bai<sup>\*</sup>

Center for Molecular Science, Institute of Chemistry, Chinese Academy of Sciences (CAS), Beijing 100080, P.R. China

Received May 9, 2003. Revised Manuscript Received August 7, 2003

The preparation and characterization of highly dispersed metal nanoparticles in porous anodic aluminum oxide (AAO) films are reported. Cross-linked polyacrylamide (PAM) hydrogel nanowires are prepared within the pores of an AAO template by electropolymerization of acrylamide. Metal nanoparticles are introduced into the polymer nanowires in the channels of AAO by a “breathing” mechanism whereby the shrunken polymer nanowires are allowed to swell in an aqueous solution containing metal nanoparticles, and the structures are then re-shrunk in acetone. The loading amount and distribution of nanoparticles in PAM nanowires can be controlled by varying the number of breathing cycles and modifying the breathing process as clearly seen in TEM images. Upon calcination, the nanoparticle/hydrogel composite results in highly dispersed metal nanoparticles supported in AAO. Au nanoparticles (~12 nm diam.) and Pt nanoparticles (~3 nm diam.) have been dispersed in PAM nanowires and the channels of AAO films and characterized by TEM, ED, SEM, and X-ray energy dispersion analysis. The assembly strategy will be useful in loading and dispersing of various nanoparticles into the channels of porous materials, as well as into the polymer nanowires.

## Introduction

Metal nanoparticles are unique materials with interesting physical and chemical properties.<sup>1,2</sup> These properties suggest enormous potential applications for metal nanoparticles as adsorbents, biological stains, elements of novel nanoscale optical, electronic, and magnetic devices, and especially novel high-efficiency chemical catalysts.<sup>3–9</sup> These distinct properties may be attributed to the quantum confinement phenomena derived from the change in the density and effective band gap of the electronic energy level as well as a high ratio of surface to bulk atoms.<sup>10</sup> Therefore, many of these proposed applications will require well dispersed nanoparticles. Unfortunately, the problem of agglomeration often exists when these metal nanoparticles are used during practical operations. However, supported metal nanoparticles highly dispersed in a host material are more desired for practical applications.<sup>11</sup>

\* To whom correspondence should be addressed. Phone and Fax: +86-10-62558934. E-mail: wanlijun@iccas.ac.cn.

<sup>†</sup> Also in Graduate School of CAS, Beijing, P. R. China.

- (1) Volokitin, Y.; Sinzig, J.; de Jong, L. J.; Schmid, G.; Vargaftik, M. N.; Moiseev, I. I. *Nature* **1996**, *384*, 621.
- (2) Lewis, L. N. *Chem. Rev.* **1993**, *93*, 2693.
- (3) Templeton, A. C.; Wuelfing, W. P.; Murray, R. W. *Acc. Chem. Res.* **2000**, *33*, 27.
- (4) Schmid, G.; Bäumle, M.; Geerkens, M.; Heim, I.; Osemann, C.; Sawitowski, T. *Chem. Soc. Rev.* **1999**, *28*, 179.
- (5) Rao, C. N. R.; Kulkarni, G. U.; Thomas, P. J.; Edwards, P. P. *Chem. Soc. Rev.* **2000**, *29*, 27.
- (6) Henglein, A. *J. Phys. Chem.* **1993**, *97*, 5457.
- (7) Jana, N. R.; Sau, T. K.; Pal, T. *J. Phys. Chem. B* **1999**, *103*, 115.

- (8) Bonnemann, H.; Braun, G. A. *Chem. Eur. J.* **1997**, *3*, 1200.
- (9) Maye, M. M.; Lou, Y.; Zhong, C.-J. *Langmuir* **2000**, *16*, 7520.
- (10) Alivisastos, A. P. *Science* **1996**, *271*, 933.

Various submicrospheres,<sup>12,13</sup> mesoporous silicas (such as MCM-41, MCM-48, and SBA-15)<sup>11,14–16</sup> and porous AAO films<sup>17</sup> are suitable supports for nanoparticles. Gedanken and co-workers used an ultrasound-driven synthesis method to deposit gold nanoparticles on the surface of preformed silica submicrospheres.<sup>12</sup> Chao and co-workers developed a method of preparing highly dispersed metal nanoparticles in functionalized mesoporous silica SBA-15.<sup>11</sup> However, the synthesis of metal nanoparticles well dispersed in porous AAO films has not been well explored. Porous AAO film has huge pore density ( $10^8$ – $10^{13}$  pores/cm<sup>2</sup>) and a larger pore size (in the range of 5–200 nm)<sup>18–22</sup> than that of MCM-41, MCM-48, and SBA-15,<sup>14–16</sup> which may facilitate the diffusion of relatively bulky molecules and the mobility

(11) Yang, C.-M.; Liu, P.-H.; Ho, Y.-F.; Chiu, C.-Y.; Chao, K.-J. *Chem. Mater.* **2003**, *15*, 275.

(12) Pol, V. G.; Gedanken, A.; Calderon-Moreno, J. *Chem. Mater.* **2003**, *15*, 1111.

(13) Wong, M. S.; Cha, J. N.; Choi, K.-S.; Deming, T. J.; Stucky, G. D. *Nano Lett.* **2002**, *2*, 583.

(14) Kresge, C.; Leonowicz, M.; Roth, W.; Vartuli, C.; Beck, J. *Nature* **1992**, *359*, 710.

(15) Zhao, D.; Feng, J.; Huo, Q.; Melosh, N.; Fredrickson, G. H.; Chmelka, B. F.; Stucky, G. D. *Science* **1998**, *279*, 548.

(16) Zhao, D.; Huo, Q.; Feng, J.; Chmelka, B. F.; Stucky, G. D. *J. Am. Chem. Soc.* **1998**, *120*, 6024.

(17) Masuda, H.; Fukuda, K. *Science* **1995**, *268*, 1466.

(18) Martin, C. R. *Science* **1994**, *266*, 1961.

(19) Miller, S. A.; Young, V. Y.; Martin, C. R. *J. Am. Chem. Soc.* **2001**, *123*, 12335.

(20) Li, A. P.; Müller, F.; Birner, A.; Nielsch, K.; Gösele, U. *J. Appl. Phys.* **1998**, *84*, 6023.

(21) Guo, Y.-G.; Wan, L.-J.; Zhu, C.-F.; Yang, D.-L.; Chen, D.-M.; Bai, C.-L. *Chem. Mater.* **2003**, *15*, 664.

(22) Guo, Y.-G.; Wan, L.-J.; Gong, J.-R.; Bai, C.-L. *Phys. Chem. Chem. Phys.* **2002**, *4*, 3422.

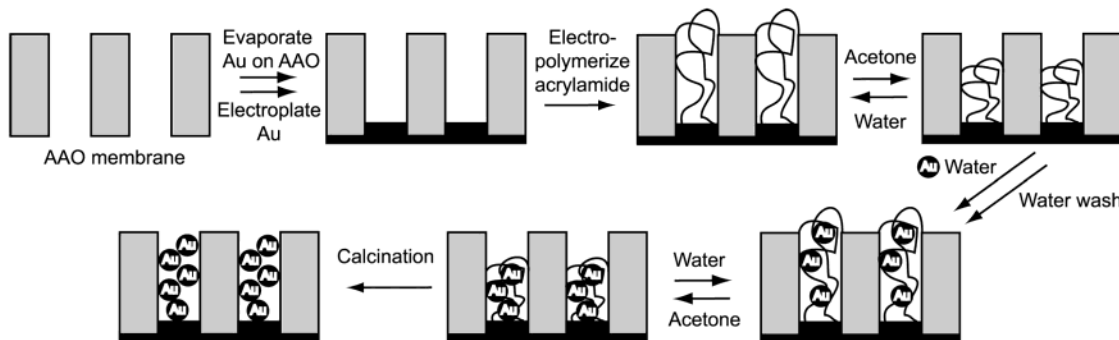


**Figure 1.** Schematic illustration for loading and dispersing Au nanoparticles into porous AAO films by a breathing process of polyacrylamide hydrogel nanowires.

of nanostructured metals. In this study, we report a novel method of preparing highly dispersed metal nanoparticles in porous AAO films.

It is well-known that polyacrylamide (PAM) hydrogels are “smart” hydrogels.<sup>23,24</sup> The PAM hydrogels adopt highly swollen structures in water, but undergo phase transitions to collapsed states upon exposure to less polar solvents such as acetone.<sup>24</sup> Willner and co-workers have successfully used this knowledge to introduce metal and semiconductor nanoparticles into the gel by a “breathing” mechanism, consisting of breathing out in an aprotic solvent and breathing in in an aqueous solution containing nanoparticles, for the fabrication of nanoparticle/hydrogel composites with interesting solvent-switchable electrical and photoelectrochemistry properties on macroscopic Au electrodes.<sup>25</sup> Here, we extend this strategy into a hydrogel-nanowire-assisted technique for the preparation of highly dispersed nanoparticles in the channels of porous AAO films as well as in the hydrogel nanowires on the motivation to address the following questions: (1) Can a hydrogel nanowire array be fabricated by electropolymerization of its monomer within the pores of an AAO membrane? (2) Does the nanoscale hydrogel still have the behavior of breathing? and (3) Can the breathing behavior be used for loading and dispersing nanoparticles into porous materials?

## Experimental Section

**Preparation of PAM Nanowire Array.** PAM nanowire array was prepared as outlined in Figure 1. Commercially available anodic aluminum oxide membranes of thickness 60  $\mu\text{m}$  and quoted pore diameter 20 and 100 nm were used as templates in our experiment. An Au film (ca. 200 nm thick Au) was deposited by vacuum evaporation onto the branched side of the AAO template to provide an electrode. The AAO template with Au substrate was used as a working electrode in a glass cell with a platinum counter electrode and a saturated calomel electrode (SCE) reference electrode. All electrode potentials here are reported with respect to the SCE. Prior to electropolymerizing acrylamide, a layer of Au segments was electroplated to fill the branched parts of the pores of AAO by using potentiostatic control at  $-0.9\text{ V}$  from the following electrolytic bath: 20 g  $\text{L}^{-1}$   $\text{HAuCl}_4 \cdot 4\text{H}_2\text{O}$ , 120 g  $\text{L}^{-1}$   $\text{Na}_2\text{SO}_3$ , 50 g  $\text{L}^{-1}$  EDTA, and 80 g  $\text{L}^{-1}$   $(\text{NH}_4)_3\text{C}_6\text{H}_5\text{O}_7$  (tri-

ammonium citrate).<sup>26</sup> After deposition, the Au-filled membrane was then exposed to the following electrolyte:  $\text{ZnCl}_2$  (0.2 M), acrylamide (5 M), and  $\text{N,N}'\text{-methylenebisacrylamide}$  (0.1 M), for the formation of PAM nanowire array. It was carried out by cyclic scanning from  $E = 0.1$  to  $-1.5\text{ V}$  (scan speed 50 mV/s), holding at  $-1.5\text{ V}$  for 20 s before commencing the next scan, for a total of 9 scans.<sup>25</sup> After electropolymerization, the array was left overnight in water to redissolve precipitated zinc, and then shrunk and swollen several times by immersion in acetone and water, respectively, to wash out impurities. Ultrapure Millipore water (Millipore-Q) was used in all experiments.

**Preparation of Au Nanoparticles.** Solutions of citrate-reduced gold nanoparticles were prepared according to the Frens method.<sup>27</sup> Briefly, 100 mL of solution containing 0.01 g  $\text{HAuCl}_4 \cdot 3\text{H}_2\text{O}$  was brought to reflux and 3 mL of 1% aqueous sodium citrate solution was added while stirring. The boiling solution was then kept for another 40 min and left to cool to room temperature. The resulting gold nanoparticle solution contained of mostly isolated, almost spherical, particles with a mean diameter of  $12 \pm 2\text{ nm}$  according to TEM. Prior to being used in the subsequent assembly processes the solution was diluted  $15\times$  using water.

**Preparation of Pt Nanoparticles.** Solutions of Pt nanoparticles were prepared by the method developed by Teranishi et al.<sup>28</sup> A mixture of 5 mL of 6.0 mM  $\text{H}_2\text{PtCl}_6$  aqueous solution (30  $\mu\text{mol}$  of Pt), 4.5 mL of water, and 40.5 mL of methanol containing 30  $\mu\text{mol}$  of poly(*N*-vinyl-2-pyrrolidone) (PVP) was refluxed in a 100-mL flask for 3 h under air to synthesize the PVP-protected Pt nanoparticles. The resulting Pt solution contained  $3 \pm 0.6\text{ nm}$  particles according to TEM and was diluted  $2\times$  with water before being used in subsequent assembly processes.

**Preparation of Nanoparticles Dispersed in Porous AAO Films.** Highly dispersed nanoparticles in porous AAO films were prepared using a hydrogel-nanowire-assisted technique as shown schematically in Figure 1. First, nanoparticles were introduced into a PAM nanowire array with AAO by a breathing mechanism consisting of three steps. (1) The swollen PAM was placed in acetone for 3 min, causing the collapse of the gel and the expulsion of water (“breathing out”). (2) The shrunken PAM was placed in the aqueous solution of Au nanoparticles or that of Pt nanoparticles for 5 min. This caused the swelling of the gel, which took in the solution (“breathing in”) including the suspended nanoparticles. (3) The PAM was washed well with water to remove weakly surface-adsorbed nanoparticles. After several cycles of the breathing process, a nanoparticle/PAM nanowire array with AAO was obtained. Highly dispersed nanoparticles in porous AAO films were produced by drying the as-prepared nanoparticle/PAM nanowire arrays at room temperature, and then calcining (heating

(23) Oya, T.; Enoki, T.; Grosberg, A. Y.; Masamune, S.; Sakiyama, T.; Takeoka, Y.; Tanaka, K.; Wang, G.; Yilmaz, Y.; Feld, M. S.; Dasari, R.; Tanaka T. *Science* **1999**, *286*, 1543.

(24) Shipway, A. N.; Willner, I. *Chem. Commun.* **2001**, 2035.

(25) (a) Pardo-Yissar, V.; Gabai, R.; Shipway, A. N.; Bourenko, T.; Willner, I. *Adv. Mater.* **2001**, *13*, 1320. (b) Pardo-Yissar, V.; Bourenko, T.; Wasserman, J.; Willner, I. *Adv. Mater.* **2002**, *14*, 670.

(26) Guo, Y.-G.; Wan, L.-J.; Bai, C.-L. *J. Phys. Chem. B* **2003**, *107*, 5441.

(27) Frens, G. *Nature* **1973**, *241*, 20.

(28) Teranishi, T.; Hosoe, M.; Tanaka, T.; Miyake, M. *J. Phys. Chem. B* **1999**, *103*, 3818.

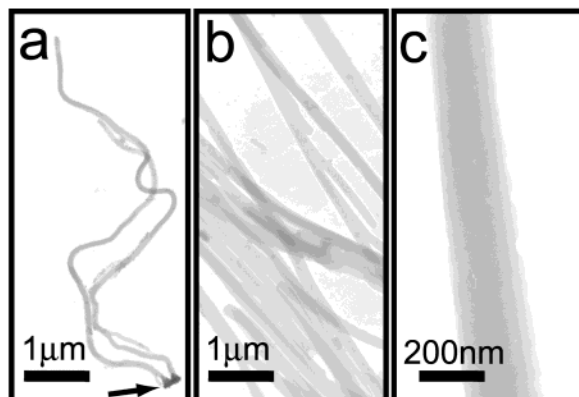


**Figure 2.** TEM images of PAM nanowires. (a) Low-magnification TEM image of shrunken PAM nanowires dispersed from acetone solution; (b) low-magnification and (c) high-magnification TEM images of swollen PAM nanowires dispersed from an aqueous solution.

rate  $10 \text{ K min}^{-1}$ ) them at  $450 \text{ }^\circ\text{C}$  under  $\text{N}_2$  for 4 h, then for a further 8 h under  $\text{O}_2$ , and then for another 8 h under  $\text{H}_2$ .

**Characterization.** The size and morphology of Au and Pt nanoparticles were observed by TEM. The samples were prepared by dropping the solution of Au or Pt nanoparticles on copper grids with carbon films.

The removal of PAM or nanoparticle/PAM nanowires from AAO matrix was carried out by dissolving the AAO template in a mixture of 6 wt %  $\text{H}_3\text{PO}_4$  and 1.8 wt %  $\text{H}_2\text{CrO}_4$  at  $25 \text{ }^\circ\text{C}$  for 3 h. For TEM observation, the nanowires were detached from the Au substrate by ultrasonic treatment and dropped on copper grids. TEM and electron diffraction were carried out with a JEM-200CX microscope operated at 160 kV and equipped with an energy-dispersive X-ray analyzer (EDAX 9100/6, Philips).

A JEOL JSM-6700F field emission scanning electron microscope was used to determine the morphology of the nanoparticles dispersed in the pores of AAO films. It was performed on the sections of film by cleaving a nanoparticle-filled AAO.

## Results and Discussion

**Morphology of PAM Nanowires.** Typical TEM images of PAM nanowires dispersed from the different solvents of acetone and water are shown in Figure 2a and 2b and c, respectively. The nanowires in Figure 2a appear to have winding shapes, while those in Figure 2b and c have straight shapes with smooth surfaces. The difference of their shapes is due to the different responses of the hydrogel in different solvents.<sup>23–25</sup> As the PAM nanowires were formed from an aqueous solution, they adopted swollen structures filling the pores of AAO, which resulted in them having the same diameters as the pores of AAO films. After removal of AAO, the PAM nanowires were dispersed from a solvent for TEM. When dispersed from acetone, the swollen PAM nanowires shrank, resulting in snaky structures with an average diameter of 110 nm, smaller than the pore diameter of AAO (Figure 2a). However, if they were dispersed from an aqueous solution, they were still the swollen structures with an average diameter of 210 nm corresponding to the actual pore diameter of the AAO template used (Figure 2b and c).

It should be noted that the diameter of the swollen wire is several times larger than the pore diameter quoted by the manufacturers (20 or 100 nm), and in fact, is close to 200 nm. According to data supplied by the manufacturer and confirmed by our own SEM studies

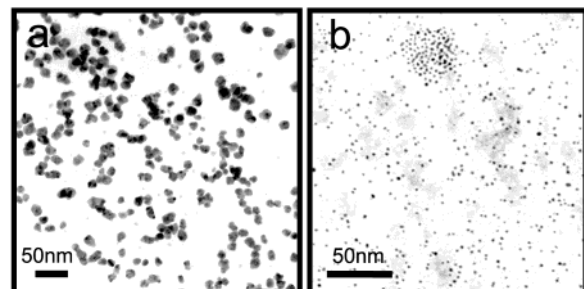


**Figure 3.** Typical TEM images of (a) Au and (b) Pt nanoparticles.

(see Supporting Information, SI 1), many pores of diameter close to the quoted value (20 or 100 nm) join to form one much larger pore within  $\sim 1 \mu\text{m}$  of the surface of the membrane that the manufacturers recommend should be uppermost for filtration applications. The change in pore diameter close to the filtration side is a consequence of a reduction in the anodization potential during manufacture.<sup>29</sup> Away from this filtration surface, the pores are straight, uniform, and parallel with a diameter of  $\sim 200 \text{ nm}$ . Therefore, the so-prepared nanowires almost have the similar diameters of  $\sim 200 \text{ nm}$  no matter which AAO template is used. Because nanoparticles will be introduced into the pores of AAO in succedent processes, the filtration side (with small mouths) should be filled with Au layer and the nonfiltration side (with large mouths) should be left open. The filling Au segments can be seen in Figure 2a indicated by an arrow.

**Morphology of Au and Pt Nanoparticles.** Figure 3a and b shows TEM images of nanoparticles corresponding to citrate-reduced Au and PVP-protected Pt, respectively, used in our assembly processes. As is evident from the figure, the images show the presence of well monodispersed nanoparticles of Au and Pt. The mean sizes of the nanoparticles are  $12 \pm 2 \text{ nm}$  for Au and  $3 \pm 0.6 \text{ nm}$  for Pt.<sup>27,28</sup>

**Morphology and Structure of Au/PAM Composite Nanowires.** As supposed in our strategy, the Au nanoparticles would be introduced into PAM if a shrunken PAM nanowire array were swelling in an aqueous solution of Au nanoparticles. Upon the next breathing out cycle, the nanoparticles remained stuck inside the PAM probably because of physical entanglement of the polymer.<sup>24,25</sup> TEM investigation provides direct observation of the morphology and distribution of Au nanoparticles in the Au/PAM composite nanowires and reveals the increasing presence of Au in the PAM with breathing cycles. Figure 4 panels a and b are the typical TEM images obtained in composite Au/PAM nanowires after eight breathing cycles between acetone and an aqueous Au nanoparticle solution. The feature of uniform nanoparticles with the same size as the citrate-stabilized 12-nm diam. Au nanoparticles highly dispersed in PAM nanowires is clearly seen in the images. This indicates that the Au nanoparticles have been successfully introduced into PAM nanowires. Further evidence can be found from the corresponding electron diffraction (ED) pattern as shown in Figure 4c. The diffraction rings and spots can be indexed as 111,

(29) Furneaux, R. C.; Rigby, W. R.; Davidson, A. P. *Nature* **1989**, 337, 147.

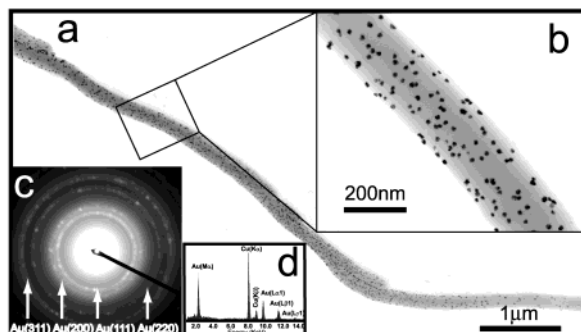


**Figure 4.** (a) Typical TEM image of Au-nanoparticle-containing PAM nanowires (eight breathing cycles between acetone and an aqueous Au nanoparticle solution) dispersed from an aqueous solution. (b) High-magnification TEM image from the framed area in Figure 4a. (c) Corresponding ED pattern and (d) EDAX profile of the composite nanowire. (Cu peaks are from the support copper grid).

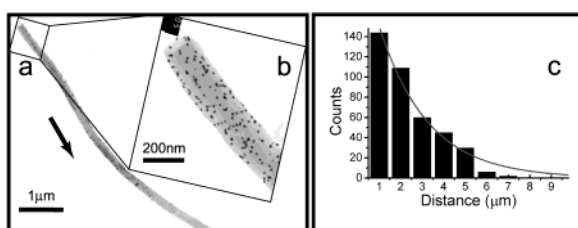


**Figure 5.** (a) Typical TEM image of an Au-nanoparticle-containing PAM nanowire (five breathing cycles between acetone and an aqueous Au nanoparticle solution) dispersed from an aqueous solution. (b) High-magnification TEM image from the framed area in Figure 5a. (c) Corresponding distribution of Au nanoparticles along the PAM nanowire in the direction as shown by the arrow in Figure 5a.

200, 220, and 311 of face-center-cubic (fcc) Au polycrystallites, which demonstrates that the particles in PAM nanowires are Au nanoparticles. As shown in Figure 4d, energy-dispersive X-ray analysis of the composite nanowire shown in Figure 4a revealed the presence of Au, also confirming the successful introduction of Au nanoparticles. In a high-magnification TEM image (Figure 4b), the average diameter of the nanowires is measured to be  $\sim 210$  nm, which is the same as that of the swollen PAM nanowire, indicating that the introduction of Au nanoparticles into PAM does not give rise to volume expansion of PAM and the introduced particles occupy only the interspace of the swollen polymer.

It should be noted that if a swollen PAM nanowire array is left in a nanoparticle solution, even for several hours, it does not absorb any nanoparticles. Thus, it is the breathing mechanism and not simple diffusion that is responsible for the nanoparticle introduction in the polymer nanowire.<sup>24,25</sup> The quantitative analysis of the Au-nanoparticles introduced into the nanowires by the breathing mechanism was further investigated by TEM.

Figure 5a and b show the typical TEM images of an Au-nanoparticle-containing PAM nanowire after five breathing cycles between acetone and an aqueous Au nanoparticle solution. Corresponding distribution of Au nanoparticles along the PAM nanowire in the direction as shown by an arrow in Figure 5a is shown in Figure 5c. An exponential decay of the introduced Au nanoparticles along the nanowire can be clearly seen, which reflects the diffuse grade of Au nanoparticles along PAM nanowires when they are breathing in. Therefore,

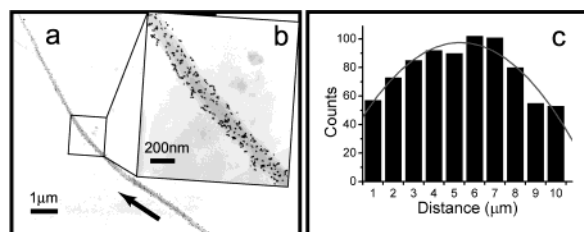


**Figure 6.** (a) Typical TEM image of an Au-nanoparticle-containing PAM nanowire (eleven breathing cycles between acetone and an aqueous Au nanoparticle solution, and then three further breathing cycles between acetone and water) dispersed from an aqueous solution. (b) High-magnification TEM image from the framed area in Figure 6a. (c) Corresponding distribution of Au nanoparticles along the PAM nanowire in the direction as shown by the arrow in Figure 6a.

increasing breathing cycles not only results in the increase of the amount of introduced Au nanoparticles, but the deeper are the Au nanoparticles diffused in PAM nanowires. Moreover, the distribution of Au nanoparticles along PAM nanowires can also be controlled by further treatments of the Au-nanoparticle-containing PAM nanowire array. Figure 6a and b show the typical TEM images of an Au-nanoparticle-containing PAM nanowire after eleven breathing cycles between acetone and an aqueous Au nanoparticle solution, and then three further breathing cycles between acetone and water. Corresponding distribution of Au nanoparticles along the PAM nanowire in the direction as shown by an arrow in Figure 6a is shown in Figure 6c. The total number of introduced Au nanoparticles in the nanowire is ca. 788, which is much increased compared to that in the nanowire in Figure 5 (ca. 396). Furthermore, the Au nanoparticles diffuse more than 11 μm along the nanowire, which is also deeper than they diffused in Figure 5 (ca. 7 μm). Because of the three further breathing cycles between acetone and water, the introduced Au nanoparticles continue to diffuse along the nanowire. Although there are no more introducing Au nanoparticles applied from solution, these treatments result in the change of the distribution of Au nanoparticles along the PAM nanowire. A distribution with maximum is developed from that of exponential decay.

**Morphology of Au Nanoparticles Dispersed in Porous AAO Films.** The as-prepared Au-nanoparticle-containing PAM nanowire array was subsequently calcined to prepare highly dispersed Au nanoparticles in porous AAO films. This was achieved by first calcining the array at 450 °C under N<sub>2</sub> for 4 h, then for a further 8 h under O<sub>2</sub>, which resulted in the decomposition and removal of PAM. A further calcining under H<sub>2</sub> was finally carried out for the reduction of Au nanoparticles, which were partially oxidized during the former calcination process. The structure and morphology of introduced Au nanoparticles along the length of the pores of AAO was determined from SEM images of films cleaved along the pore axis. The typical images of Au nanoparticles within the AAO film are shown in Figure 7a–d. A large number of Au nanoparticles dispersed in the parallel channels of AAO is clearly seen in the images. The absence of Au nanoparticles along a channel of the AAO film resulting from the cleaving process is also visible, as indicated by the arrow in Figure 7d. The nanoparticles in Figure 7 are larger than

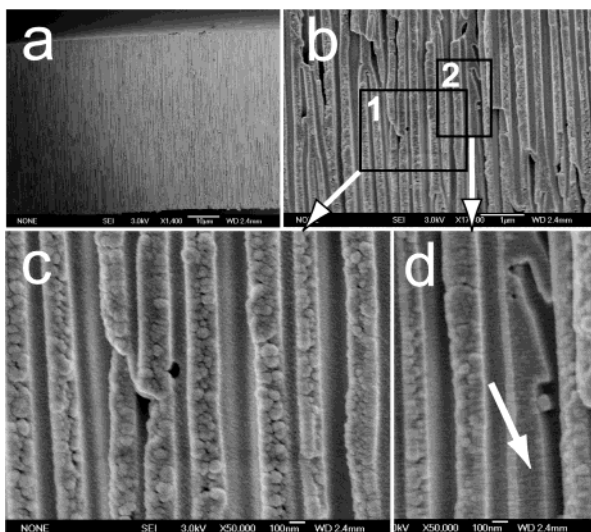


**Figure 7.** Cross-section SEM images of an AAO film containing Au-nanoparticle/PAM after calcination treatments: (a) whole and (b) part views of the cross-section; (c) and (d) high-magnification SEM images from the framed areas of 1 and 2 in Figure 7b, respectively.

the original citrate-stabilized 12-nm-diam Au nanoparticles, which can be attributed to (1) a platinum film which was evaporated onto the specimen before imaging to prevent charging effects and (2) a slight aggregation of Au nanoparticles that occurred upon calcination due to the removal of the protecting layer and the fusion of particles. Well dispersed nanoparticles can be obtained by decreasing the loading-amount of Au nanoparticles. Furthermore, a novel nanoparticle wire is constructed when the loading-amount of nanoparticles is very large. As the incorporation of semiconductor nanoparticles in PAM by the breathing mechanism has been described,<sup>25</sup> the reported method has potential extension to the preparation of semiconductor nanoparticle wires.

**Dispersion of Pt Nanoparticles.** The strategy of loading nanoparticles into porous AAO membranes by the breathing process of PAM hydrogel nanowire array has also been extended to introduce other metal nanoparticles. The requirement seemed to be that these metal nanoparticles should be dispersed in an aqueous solution, even a mixed solvent containing mainly water. For example, Pt nanoparticles could be introduced into AAO films when a PAM nanowire array with AAO is breathing between acetone and a solution of Pt nanoparticles in a mixed solvent of methanol/water (9:11). Typical TEM images of Pt-nanoparticle-containing PAM nanowires after three breathing cycles are shown in the Supporting Information (SI 2). The high-magnification TEM image of SI 2b clearly shows uniform and highly dispersed Pt nanoparticles with the same size as the PVP-protected 3-nm-diam Pt nanoparticles in the PAM

nanowires. A corresponding ED pattern of the composite nanowires is shown in SI 2c. The diffraction rings and spots can be indexed as 111, 200, 220, and 311 of fcc Pt polycrystallites. This verifies that the particles in the PAM nanowires really are Pt nanoparticles. The successful introducing of Pt nanoparticles into PAM nanowires indicates that the PAM hydrogel also adopts a swollen structure in the water-containing mixed solvent of methanol/water (9:11). Pt nanoparticles dispersed in the channels of porous AAO films can also be obtained after the same calcination treatment as that applied for Au nanoparticles.

## Conclusion

In summary, we have demonstrated a simple and versatile route to highly disperse nanoparticles in porous AAO films using a hydrogel-nanowire-assisted technique. First, a nanoparticle/PAM composite nanowire array was prepared from a template-grown PAM hydrogel nanowire array based on a breathing mechanism. Then, calcining was applied for the removal of the hydrogel media and resulted in highly dispersed nanoparticles in porous AAO films. The advantage of the hydrogel-nanowire-assisted approach over other methods is that the loading amount and distribution of nanoparticles in the hydrogel nanowires or the channels of AAO films can be easily controlled by varying the number of breathing cycles and modifying the breathing process, respectively. Furthermore, this information can be clearly seen in the TEM images of their nanoparticle/hydrogel nanowire precursor. The major requirement of this approach is the availability of nanoparticles that can be dissolved in water or water-containing solvent. Given the fact that most metals and semiconductors have already been synthesized into nanoparticles, the number of nanoparticles that can be introduced into porous AAO films using this approach is potentially very large. Because of the well-controlled loading amount and distribution of nanoparticles in AAO films and PAM nanowires, these nanoparticle/AAO or nanoparticle/PAM nanowire composites will find use in a number of applications that involve sensing and catalysis.

**Acknowledgment.** We thank the National Natural Science Foundation (20025308, 20177025, 10028408, and 20121301) and the Chinese Academy of Sciences for financial support. Support from the National Key Project on Basic Research (grant G2000077501) is also acknowledged.

**Supporting Information Available:** TEM images of porous AAO films and Pt-nanoparticle-containing PAM nanowires. This material is available free of charge via the Internet at <http://pubs.acs.org>.

CM0343397